

## A Control Algorithm for Optimal Energy Performance of a Solarium/Greenhouse with Combined Interior and Exterior Motorized Shading

Bastien, Diane; Athienitis, Andreas K

*Published in:*  
Energy Procedia

*DOI:*  
[10.1016/j.egypro.2012.11.112](https://doi.org/10.1016/j.egypro.2012.11.112)

*Publication date:*  
2012

*Document version:*  
Final published version

*Document license:*  
CC BY-NC-ND

*Citation for pulished version (APA):*  
Bastien, D., & Athienitis, A. K. (2012). A Control Algorithm for Optimal Energy Performance of a Solarium/Greenhouse with Combined Interior and Exterior Motorized Shading. *Energy Procedia*, 30, 995-1005. <https://doi.org/10.1016/j.egypro.2012.11.112>

Go to publication entry in University of Southern Denmark's Research Portal

### Terms of use

This work is brought to you by the University of Southern Denmark.  
Unless otherwise specified it has been shared according to the terms for self-archiving.  
If no other license is stated, these terms apply:

- You may download this work for personal use only.
- You may not further distribute the material or use it for any profit-making activity or commercial gain
- You may freely distribute the URL identifying this open access version

If you believe that this document breaches copyright please contact us providing details and we will investigate your claim.  
Please direct all enquiries to [puresupport@bib.sdu.dk](mailto:puresupport@bib.sdu.dk)

SHC 2012

## A control algorithm for optimal energy performance of a solarium/greenhouse with combined interior and exterior motorized shading

Diane Bastien<sup>a,\*</sup>, Andreas K Athienitis<sup>a</sup>

<sup>a</sup>Concordia University, 1455 de Maisonneuve Blvd. West, Montréal H3G 1M8, Canada

---

### Abstract

A solarium/greenhouse attached to a building can provide many benefits, such as collecting solar energy, allowing the cultivation of plants and providing an enjoyable living space to its occupants. Integrating moveable shading devices with fenestration is a recognized way to reduce heat losses and control solar gains. The control strategy for operating shades can have a significant impact on the energy performance of fenestration systems.

The aim of this study is to develop an algorithm for the optimum control of combined interior and exterior motorized shading devices based on an energy balance method. The algorithm developed here is designed to maximize solar heat gains while reducing heat losses during the heating season for a cold climate. An attached solarium with motorized shading devices located in Montreal is simulated during the heating season. Results show that heating requirements can be reduced by up to 76% using the proposed algorithm compared to a control scheme based on a fixed solar radiation level. The solarium could collect up to 3.2 MWh (or 134 kWh/m<sup>2</sup> of floor area) of excess heat that could be supplied to the house during the heating season. This algorithm could be useful especially in solariums/greenhouses and could be of interest also for solar houses and high efficiency buildings when increasing solar gains and reducing heat losses is a priority.

© 2012 The Authors. Published by Elsevier Ltd. Open access under [CC BY-NC-ND license](https://creativecommons.org/licenses/by-nc-nd/4.0/).  
Selection and/or peer-review under responsibility of PSE AG

*Keywords:* Solarium; greenhouse; energy balance; optimum control strategy; motorized shading; roller blind, roller shutter

---

---

\* Corresponding author. Tel.: +1-514-848-2424 #7244; fax: +1-514-848-7965.  
E-mail address: [solarbuildings@dianebastien.ca](mailto:solarbuildings@dianebastien.ca).

## 1. Introduction

The addition of a solarium attached to a house or a rooftop greenhouse can provide many benefits such as collecting solar energy, allowing the cultivation of plants and providing an enjoyable additional space for the occupants. Thermal energy can be transferred from a solarium/greenhouse to its adjacent building and therefore supply a fraction of its heating needs. The use of movable shading devices in highly glazed spaces can affect significantly solar gains and heat losses through the fenestration.

Usually, for heating dominated buildings, only fenestration facing close to the equator gather more energy than they lose, while fenestration at other orientations is usually a net energy loser. However, it has been found that the overall energy impact of a window of average orientation can be approximately zero if  $1.7 \text{ m}^2\text{K/W}$  (R10) shutters are used twelve hours a day with clear double-glazing in a severe climate (Minneapolis, Minnesota) [1].

The operating conditions of shading devices have a significant impact on the energy consumption of buildings. Numerous studies have been conducted about the operation of different types of movable shading devices and the energy performance of office buildings, especially impacts related to heating and cooling loads, artificial lighting and visual comfort (workplane illuminance and glare issues) [2–4].

While being important for non-residential buildings, the use of movable shading devices becomes essential for greenhouses and solariums. Practically entirely glazed, structures of this kind are subjected to extreme solar gains and heat losses. This is why the use of movable shading devices, also known as thermal screens, are under intensive study in the field of protected cultivation since the 80's.

Needs differ greatly between commercial greenhouses and office buildings. For the first one, control of movable shading devices is based on maximizing solar radiation transmission and minimizing heat losses (to maximize crop production and reduce heating needs) while for the latter it is based on minimizing air conditioning and heating, reducing electric lighting and controlling glare. Control strategies for operating thermal screens in greenhouses can be based on several approaches such as:

- Time clock operation;
- A fixed value of solar irradiance;
- A linear correlation between solar irradiance and outside temperature;
- An economic criteria based on energy saved versus crop lost;
- An energy balance on the glazing.

It was found that energy savings can be increased by 6% when the screen is controlled based on radiation level compared to time clock operation [5]. Marsh, Albright & Langhans [6] measured an energy saving of 3.3% when the opening of thermal screens was based on an inside light level of  $30 \text{ W/m}^2$  compared to time clock operation. This study also concluded that using a more complicated control strategy based on a light level that is a linear function of the outside temperature is not justified because no additional savings were observed compared to a fixed light level control.

Nowadays, with the widespread availability of solar radiation sensors and their relatively low cost and ease of use, controls based on a fixed value of solar radiation should be preferred to time clock operation to increase energy savings. Simulations carried out by Dieleman & Kempkes [7] have shown that by operating a thermal screen opening based on outside radiation level from  $1 \text{ W/m}^2$  to 25, 50 and  $150 \text{ W/m}^2$ , an additional energy saving of 2%, 3% and 4% respectively can be achieved. The same study found that operating the screen based on correlations of outside temperature and radiation can achieve a similar energy reduction of up to 4% compared to an operation strategy based on a fixed outside radiation level of  $1 \text{ W/m}^2$ .

A previous study on the optimum control of a motorized interior roller blind based on an energy balance on the glazing was conducted [8]. It was found that, depending of the properties of the roller

blind, the heat balance control method could reduce the heating requirements by up to 37% compared to control methods based on a fixed radiation set point, below which a blind is closed. Maximum reduction of heating needs occurred when using a low emissivity opaque roller blind. However, by using a high transmittance screen controlled with a heat balance method, simulations found that up to 122% additional heat could be stored.

## 2. Problem statement and objectives

While using multiple thermal screens has been identified by many as a promising way to reduce heat losses through glazings [9–11], the authors are not aware of any published studies concerning the optimum control of multiple motorized shading devices for reducing overall heat losses. A promising combination of shadings consists of one opaque insulated exterior shutter and one interior high transmittance roller blind. The roller shutter is likely to be used at night when there is no solar radiation while a screen with high transmittance can be used on cold days to permit good solar radiation transmission while reducing heat losses simultaneously.

The aim of this study is to develop an algorithm for the optimum control of interior and exterior motorized shading devices based on an energy balance method and assess its energy saving potential. Simulation results presented in this paper compare the heating needs and the excess heat that can be stored in an attached solarium with no shades, with an exterior roller shutter, with an interior roller blind and with both interior and exterior shades combined. The effect of growing plants in the solarium is also investigated. Because façades with different orientations are subjected to varying solar gains, shades on surfaces with different orientation can be controlled individually.

The operating strategy of shadings with the energy balance method developed here is compared with controls based on a fixed set point of outdoor solar radiation. This work may be useful not only for attached solariums and commercial greenhouses but also for residential and high performance buildings when maximizing solar gains and minimizing heat losses is the primary concern.

## 3. Methodology

### 3.1. Geometrical parameters and material properties

A 10 m long by 2.4 m wide solarium attached to a house is simulated using a custom model developed in Matlab [12]. The solarium is facing due south; the 35° south roof and the south, east and west façades are fully glazed. Figure 1 depicts the geometry of the attached solarium. The common wall between the solarium and the house is made of 20 cm of concrete (without insulation) and a large glazed door. The temperature in the adjacent house is assumed to be constant at 20°C. The floor is made of 50 cm of soil exposed to the sun.

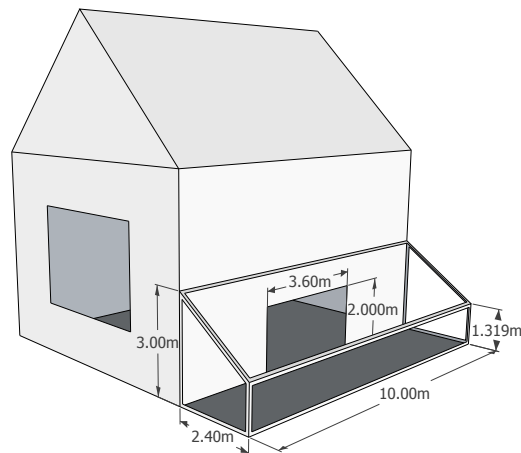


Fig. 1. Attached solarium with a roof tilt angle of 35°

The Insulated Glazed Unit (IGU) has a thickness of 13 mm and two panes of clear glass (rated U-value of 2.74 W/(m<sup>2</sup>K)). The solar transmittance at normal incidence is equal to 0.703. The optical properties of the IGU (transmittance and absorptance) at different incidence angles (90°, 80°, ..., 0°) were calculated by WINDOW 6.3 [13] and imported into the simulation model. Polynomial interpolation was used in order to calculate the optical properties for incidence angles of any discrete value. The fiberglass frame has a U value of 1.7 W/(m<sup>2</sup>K) and is assumed to represent 15% of the window area.

The four exterior glazed surfaces (east, west, vertical south and tilted south) may be equipped with an exterior roller shutter and/or an interior roller blind. The opaque roller shutter has a thermal resistance of 0.1 Km<sup>2</sup>/W (which is a typical value for commercial PVC shutters) and an emissivity of 0.8 while the roller blind has a transmittance of 0.7 and an emissivity of 0.8. The air cavity between the exterior shade and the window is 5 cm wide while the air cavity between the indoor shade and the window is 3 cm wide.

### 3.2. Model inputs and simulation details

The inputs of the model are read from the Canadian Weather year for Energy Calculation (CWEC) file for Montreal and consist of the following: global horizontal radiation, direct normal radiation, diffuse horizontal radiation, wind speed, outdoor temperature and relative humidity. Hourly values are read and then interpolated to fit the chosen time step.

Calculations are performed following a thermal network approach in which transient effect induced by thermal mass are adequately modeled by including a capacitance term:

$$T_{i,t+1} = \frac{\Delta t}{C} (q_i + \sum_j (T_{j,t} - T_{i,t}) U_{i,j}) + T_{i,t} \quad (1)$$

where  $\Delta t$  is the time step (for this study, 12mn was selected since it offered a satisfactorily trade-off between computation time and stability),  $C$  is the capacitance at node  $i$ ,  $q_i$  is a heat source absorbed at node  $i$ ,  $T_i$  is the temperature at node  $i$  and  $U_{i,j}$  is the overall conductance between nodes  $j$  and  $i$ .

### 3.3. Solar radiation transmission and distribution

For highly glazed spaces, only 30% to 90% of transmitted solar radiation is typically retained in the space, the remaining being lost to outside [14]. Therefore, for such spaces, it is necessary to simulate the distribution of solar radiation carefully. In the present model, the solar radiation distribution inside the solarium is simulated by combining ray tracing and radiosity methods.

To find the portion of a window which is illuminating directly a surface, the coordinates of that surface need to be projected onto the window plane along the sun ray employing a homogenous coordinate method. A method to calculate the homogenous coordinates and the area of overlapping convex polygons is given in [15].

The solar radiation absorbed by interior surfaces of the room is calculated following the procedure developed in [16] and [17]. The total beam radiation  $S_{b,i}$  absorbed by a surface  $i$  is given by

$$S_{b,i} = \alpha_i G_b f_{w,i} + A_i \sum_j \frac{F_{ij}^d \rho_j G_b f_{w,j}}{A_j} \quad (2)$$

where  $\alpha_i$  and  $A_i$  are the absorptance and area of surface  $i$ ,  $f_{w,i}$  is the part of the window area illuminating directly surface  $i$ ,  $F_{ij}^d$  is a transfer factor and  $\rho_j$  is the reflectance of surface  $j$ .  $G_b$  and  $G_d$  are the transmitted beam and diffuse solar radiation respectively. The diffuse solar radiation  $S_{d,i}$  transmitted through a window and absorbed by surface  $i$  is calculated with

$$S_{d,i} = A_i G_d F_{i,w}^d \quad (3)$$

Additional simulation details regarding the simulation of solar radiation distribution can be found in [18].

### 3.4. Long wave radiation exchanges

Long wave radiation exchanges between interior surfaces are modelled using the Gebhart method. The net radiation flux emitted by a surface ( $i$ ) with emittance ( $\epsilon$ ) is therefore calculated as

$$Q_{rad,i} = \epsilon_i A_i \sigma \sum_{j=1}^n G_{ij} (T_i^4 - T_j^4) \quad (4)$$

where  $\sigma$  is the Stefan-Boltzmann constant,  $n$  is the number of surfaces and  $G_{ij}$  is a Gebhart coefficient. The  $n^2$  Gebhart coefficients, which depend on the geometry and thermal properties of the surfaces, can be calculated from [19]. Radiation exchange between an exterior surface and the sky is given by

$$Q_{rad} = \epsilon_i A_i \sigma (T_i^4 - T_{sky}^4) \quad (5)$$

where the sky temperature is calculated from the atmospheric temperature as suggested in ASHRAE Applications Handbook [20].

The thermal resistance of glazing and shading systems are calculated individually at every time step to take into account variations due to temperature. Radiative heat transfer between panes of glass and window/shade cavities are calculated based on the fundamental equation for two infinite parallel plates.

### 3.5. Convective heat transfer coefficients

Local convective coefficients of interior surfaces are calculated individually as a function of surface and air temperature difference. Correlations for convective coefficients of interior building surfaces for vertical glazing (with no radiator under the window), vertical wall and horizontal surface (facing upward) developed by Khalifa and Marshall [21] are employed. The convective coefficient due to wind effect on buildings is calculated by using the recommended equation given in Duffie and Beckman [22].

Convective coefficients for air spaces between window panes and between windows and shading devices are calculated following the procedure outlined in ISO 15099 [23] for thermally driven ventilation. The convective coefficient in a ventilated gap is given by

$$h_c = 2h_{c,nv} + 4v \quad (6)$$

where  $h_{c,nv}$  is the convective coefficient for non-vented cavities and  $v$  is the mean air velocity (in m/s) in the gap. More details about the procedure for calculating  $h_{c,nv}$  and  $v$  can be found in [24].

### 3.6. Indoor conditions

Simulations are performed with and without the presence of plants. In the presence of plants, it is assumed that 80% of the floor area is covered by plants and that 50% of the solar radiation absorbed by the floor is used for evapotranspiration, as suggested by Hellickson and Walker [25]. In addition, the indoor relative humidity is kept constant at 75% and controlled by a heat recovery ventilator with 80% efficiency when the presence of plants is simulated. Occasionally, when the outdoor air has very high water vapor content, the indoor humidity may be higher than 75%. The maximum ventilation rate is set to 7 air changes per hour (ACH) to avoid losing too much heat for humidity control. When there are no plants, there is no active ventilation: air exchange occurs only through infiltration, which is assumed to be equal to 1 ACH. Heating is provided to keep a minimum air temperature of 10°C, which is deemed acceptable to avoid any frost problems. The maximum temperature allowed in the greenhouse is 28°C; this excess energy, that can be stored, transferred to the house, or vented outdoors (and therefore lost), is compiled and presented along with the heating requirements. These setpoints were chosen to limit heating requirements, overheating and potential plants damages but also to allow a wide temperature swing to foster the efficiency of the solarium/greenhouse as a solar collector.

Plants transpiration is proportional to both solar radiation and water vapor difference between saturated and unsaturated inside air. It is modeled following the general form of the Penman-Monteith equation [26]. Additional simulation details related to plants transpiration are given in [27].

### 3.7. Control algorithms

Interior and exterior shadings are motorized and can be controlled individually depending on their orientations. The main objective of this study is to compare different types of controls for motorized shadings and assess their relative energy performance. The proposed control based on a heat balance on windows is compared with control schemes based on a fixed solar radiation setpoint. Two situations are considered for the latter: when shades are controlled together based on the value of the global horizontal radiation and when shades are control individually based on the value of the incident solar radiation on a specific surface.

In the EnergyPlus [24] building simulation software, the total heat flow through a window is defined as:

- Solar radiation transmitted through the window
- + Convective heat flow from the inside glazing to the zone
- + Net IR heat flow from the inside of the glazing to the zone
- - Short wave radiation from zone transmitted back out of the window
- + Conduction from window frame and divider to the zone

The term short wave radiation refers to radiation emitted by lights and the diffuse interior solar radiation. If an interior shade is present, the heat flow calculations are carried out between the interior surface of the shade and the zone. In addition, the following term must be added:

- + Convective heat flow from air flowing in the gap between the interior glazing and shade to the zone

In the simulations undertaken for this study, the first and the fourth terms are combined and replaced by the solar radiation transmitted through the window and absorbed by interior surfaces, which takes into account the diffuse solar radiation that is reflected back to windows and transmitted outside. No artificial lights are considered in this study.

The total heat flow through a window defined here is very sensitive to the convective heat flow from the inside glazing to the zone. Opening or closing an interior shade causes an abrupt change of temperature of the innermost layer. Consequently, the total heat flow calculated in this way changes suddenly at the opening or closing of an interior shade, which makes it difficult to control the shades efficiently and smoothly. Therefore, in the frame of this study, the total heat flow through a window is calculated based on the overall heat transfer coefficient (U value) and the temperature difference between indoor and outdoor. The overall heat transfer coefficient is calculated based on the convection and radiation exchanges in glass and/or shades cavities and the indoor and outdoor convective coefficients. Conduction through the frame is also accounted for by using the parallel path heat flow method. Consequently, the total heat flow through a window is calculated as:

- Solar radiation transmitted through the window and absorbed by interior surfaces
- + Heat flow through the window from outdoor to the zone
- + Net IR heat flow from the inside of the glazing to the zone
- + Convective heat flow from air flowing in the gap between the interior glazing and shade to the zone (if an interior shade is present)

More specifically, the total heat flow through a window with/without shades is given in Table 1:

Table 1. Total heat flow through fenestration system with interior and/or exterior shades

Type of shades	Total heat flow through fenestration system
Window without shades	$Q_{no\_shade}(i) = S_{no\_shade}(i) - U_{no\_shade} * A * (T_i(i) - T_o(i)) - Q_{rad,no\_shade}(i)$
Window with interior shade	$Q_{int\_shade}(i) = S_{int\_shade}(i) - U_{int\_shade} * A * (T_i(i) - T_o(i)) - Q_{rad,int\_shade}(i) + Q_{vent}(i)$
Window with exterior shade	$Q_{ext\_shade}(i) = S_{ext\_shade}(i) - U_{ext\_shade} * A * (T_i(i) - T_o(i)) - Q_{rad,ext\_shade}(i)$
Window with interior and exterior shades	$Q_{int+ext\_shade}(i) = S_{int+ext\_shade}(i) - U_{int+ext\_shade} * A * (T_i(i) - T_o(i)) - Q_{rad,int+ext\_shade}(i) +$

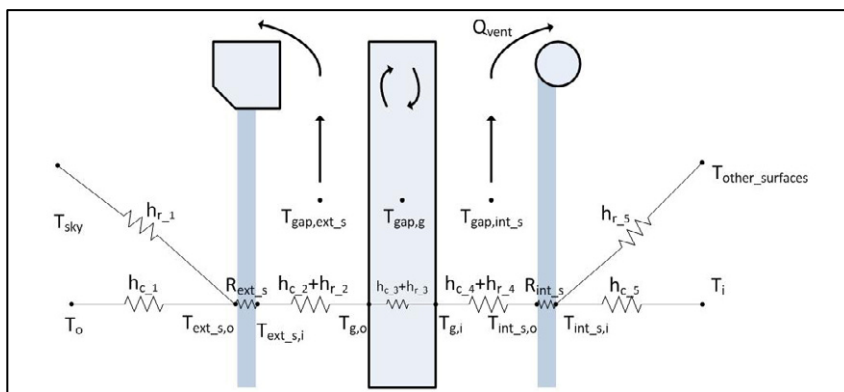


Fig. 2. Thermal network of fenestration system



A thermal network showing the conductive, radiative and convective heat transfers in the fenestration system considered in this study is shown in Figure 2. Convective and radiative coefficients  $h_{c_i}$  and  $h_{r_i}$  are calculated individually like described in the previous sections.

Although in general, shades can be totally open, totally closed, or partially open, only the two limiting cases are considered here. This is because we are interested primarily in reducing heat losses and maximizing heat gains, therefore the optimal position of a shade would be either totally open or closed. For a real life application (for controlling shades in a solarium or a house), the authors suggest that the control algorithm be implemented to control motorized shades as the default mode but occupants override should be allowed. Therefore, the results presented in this study should be seen as “best case scenario” or “maximum energy saving” since it is expected that occupant comfort/needs would sometimes supersede energy efficiency concerns.

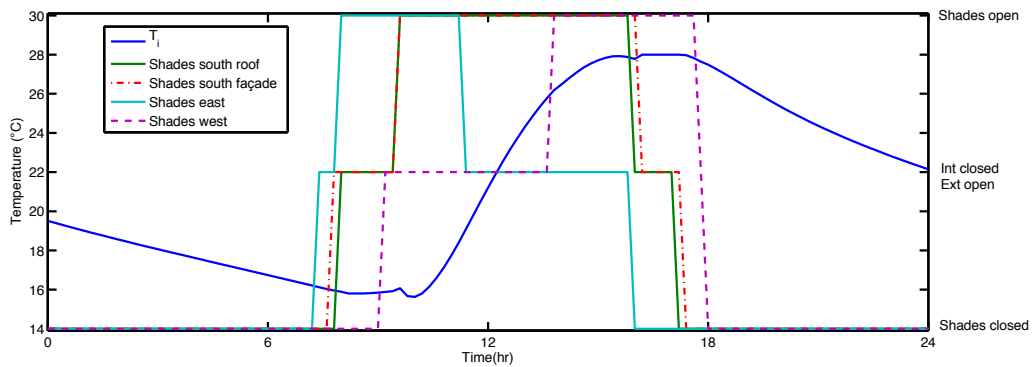
#### 4. Results

Simulations of solarium/greenhouse attached to a house are performed for a severe climate (Montreal) during the heating season. An energy efficient design was selected with the goal of collecting extra heat that could be used to heat the adjacent house. Simulations were carried out from September 1<sup>st</sup> to April 28<sup>th</sup>, but only results from October 1<sup>st</sup> to April 28<sup>th</sup> are presented (the month of September being used to provide adequate initial conditions). The heating set point is 10°C and the maximum temperature allowed inside the greenhouse is 28°C; whenever this happened, the excess heat was compiled. This extra heat could eventually be stored, transferred to the house or simply vented to outside by ventilation. The energy control algorithm is detailed in the previous section. Two types of solar controls are investigated: the so-called global solar control and the individual solar control. For the global solar control, shades from all

Table 2. Heating requirements, excess energy and average temperature of an attached solarium with and without plants and with different shade configurations and controls from October 1<sup>st</sup> to April 28<sup>th</sup> (setpoints: 10°-28°).

Type of control	Heating requirements (kWh)	Excess energy (kWh)	Average temperature (°C)
<b>Windows without shades-Without plants</b>			
No shades	2279	841	14.89
<b>Windows with interior shade-Without plants</b>			
Energy balance control	583	2334	19.26
Global solar control (150W/m <sup>2</sup> )	830	1292	17.89
Global solar control (250W/m <sup>2</sup> )	867	1381	18.07
Individual solar control (150W/m <sup>2</sup> )	786	1329	18.01
Individual solar control (250W/m <sup>2</sup> )	767	1529	18.32
<b>Windows with exterior shade-Without plants</b>			
Energy balance control	372	1797	18.68
Global solar control (50W/m <sup>2</sup> )	521	1174	17.54
Global solar control (150W/m <sup>2</sup> )	609	1178	17.60
Individual solar control (150W/m <sup>2</sup> )	482	1211	17.74

Individual solar control (200W/m <sup>2</sup> )	506	1228	17.80
<b>Windows with interior and exterior shades-Without plants</b>			
Energy balance control	55	3209	21.51
Global solar control (ext: 50W/m <sup>2</sup> , int: 150W/m <sup>2</sup> )	238	1494	19.14
Global solar control (ext: 50W/m <sup>2</sup> , int: 200W/m <sup>2</sup> )	229	1561	19.34
Individual solar control (ext: 50W/m <sup>2</sup> , int: 100W/m <sup>2</sup> )	278	1420	18.87
Individual solar control (ext: 50W/m <sup>2</sup> , int: 150W/m <sup>2</sup> )	285	1456	18.99
<b>Windows without shades-With plants</b>			
No shades	2722	404	14.05
<b>Windows with interior shade-With plants</b>			
Energy balance control	610	1579	18.72
Individual solar control (250W/m <sup>2</sup> )	1003	830	17.35
<b>Windows with exterior shade-With plants</b>			
Energy balance control	366	1153	18.12
Individual solar control (150W/m <sup>2</sup> )	682	632	16.68
<b>Windows with interior and exterior shades-With plants</b>			
Energy balance control	104	2061	20.50



Global solar control (ext: 50W/m <sup>2</sup> , int: 200W/m <sup>2</sup> )	350	820	18.24
--	-----	-----	-------

Fig. 3. Temperature inside the solarium and operation of shades with the energy balance control algorithm on February 13.

orientations are controlled together based on the global horizontal radiation level. For the individual solar control, shades with different orientations are controlled independently based on their respective incident solar radiation level. Many simulations were run with different solar radiation setpoints, but only the best results are presented in Table 2. Therefore, these radiation setpoints can be considered as near optimum.

The heating requirements, excess heat and average indoor temperature in the solarium are presented in Table 2 for a solarium with and without plants. It can be seen that a solarium/greenhouse equipped with an interior and/or exterior shade controlled with the proposed method could collect from 1.1 to 3.2 MWh (or 48-134 kWh/m<sup>2</sup> of floor area) that can be used to supply heat to the attached house during the heating season. The inside temperature and the position of shades when controlled by the energy balance algorithm are depicted in Figure 3 for a cold sunny day on February 13.

## 5. Conclusion

A control algorithm for operating motorized shadings for minimizing heat losses and maximizing solar gains is developed and presented in this paper. Heating requirements and excess energy collected by an attached solarium equipped with motorized interior and/or exterior shading devices are presented for the heating season in a cold climate (Montreal). Simulations of a solarium equipped with an insulated exterior roller shutter and an interior roller blind controlled with the proposed algorithm has shown to require virtually no heating to maintain a minimum temperature of 10°C and to collect up to 3,2 MWh of heat (or 134 kWh/m<sup>2</sup> of floor area) that could be supplied to the adjacent house. When compared with the best solar control, heating requirements are reduced by 76% and the excess heat collected is increased more than twice. Even when plants are grown in the solarium, simulations have shown that heating requirements can be reduced by 70%.

Further studies will investigate the thermal performance of interior and exterior motorized shades for different glazing types (double/triple, with argon/low e, etc...). Another next step is to develop a simpler algorithm that could be used for real time control. Transfer functions are suitable for this application because they can provide reasonably good accuracy with few inputs. Transfer functions for the optimal control of motorized shadings for minimizing heat losses through fenestration systems will be derived for real time control of motorized shades for different cases considering varying amount of thermal storage.

## Acknowledgements

The first author would like to acknowledge support from the Fonds de recherche du Québec – Nature et technologies (FQRNT) for a Doctoral Research Scholarship and Concordia University for a Special Scholarship for New High-Caliber PhD Students, as well as partial support from the NSERC Smart Net-zero Energy Buildings Strategic Research Network.

## References

- [1] Selkowitz S. E., and Bazjanac V., 1979, "Thermal performance of managed window systems," Lawrence Berkeley Laboratory Report LBL-9933, Orlando, p. 19.
- [2] Wienold J., 2007, "Dynamic Simulation of Blind Control Strategies for Visual Comfort and Energy Balance Analysis," Building Simulation, pp. 1197-1204.
- [3] Athienitis A. K., and Tzempelikos A., 2002, "A Methodology for Simulation of Daylight Room Illuminance Distribution and Light Dimming for a Room with a Controlled Shading Device," Solar Energy, **72**(4), pp. 271-281.
- [4] Carbonari A., Rossi G., and Romagnoni P., 2001, "Optimal Orientation and Automatic Control of External Shading Devices in Office Buildings," 18th Conference on Passive and Low Energy Architecture, Florianópolis, pp. 1-12.
- [5] Seginer I., and Albright L., 1980, "Rational operation of greenhouse thermal curtains," Transactions of the {ASABE}, **23**(5), pp. 1240-1245.
- [6] Marsh L., Albright L., and Langhans R., 1984, "Strategies for controlling greenhouse thermal screens," Acta Horticulturae, **148**, pp. 453-460.

- [7] Dieleman J., and Kempkes F., 2006, "Energy screens in tomato: determining the optimal opening strategy," *Acta Horticulturae*, **718**, pp. 599-606.
- [8] Bastien D., and Athienitis A. K., 2011, "Control Strategy for Thermal Screens in Greenhouse : an Algorithm Based on Heat Balance," *Acta horticulturae*, (To be published).
- [9] Meyer J., 2011, "Extremely Insulated Greenhouse Concept with non fossil Fuel Heating System," *Acta horticulturae*, **893**(201-208).
- [10] Tantau H.-J., Meyer J., Schmidt U., and Bessler B., 2011, "Low Energy Greenhouse – a System Approach," *Acta horticulturae*, (893), pp. 75-84.
- [11] Farrell J., Albright L., and Donohoe L., 1980, "A highly insulative thermal curtain for greenhouses," *ASAE*, **80**, p. 38.
- [12] MathWorks T., 2011, *Matlab R2011b*.
- [13] LBNL, 2011, "WINDOWS 6.3."
- [14] Wall M., 1995, "A Design Tool for Glazed Spaces. Part I: Description.," *ASHRAE Transactions* 101, pp. 1261-1271.
- [15] Walton G. N., 1979, "The application of homogeneous coordinates to shadowing calculations," *ASHRAE Transactions* 79, pp. 174-179.
- [16] Athienitis A. K., and Sullivan H. F., 1985, "Efficient method for determination of solar radiation absorbed by each room interior surface, and effects," *International Solar Energy Society*, Pergamon Press, pp. 430-434.
- [17] Athienitis A. K., and Stylianou M., 1991, "Method and global relationship for estimation of transmitted solar energy distribution in Passive Solar Room," *Energy Sources*, **13**, pp. 319-336.
- [18] Bastien D., and Athienitis A. K., 2010, "Analysis of the Solar Radiation Distribution and Passive Thermal Response of an Attached Solarium / Greenhouse," *International High Performance Buildings Conference*, Purdue University, pp. 1-8.
- [19] Siegel R., and Howell J. R., 1981, *Thermal radiation heat transfer*, Hemisphere Publishing Corporation.
- [20] ASHRAE, 2007, "HVAC Applications," A33, p. p6.
- [21] Khalifa A., and Marshall R., 1990, "Validation of heat transfer coefficients on interior building surfaces using a real-sized indoor test cell," *International Journal of Heat and Mass Transfer*, **33**(10), pp. 2219-2236.
- [22] Duffie J. A., and Beckman W. A., *Solar engineering of thermal processes*, 3rd edition, John Wiley & Sons, p.166.
- [23] ISO 15099, 2003, "Thermal performance of windows, doors and shading devices - Detailed calculations," p. 71.
- [24] LBNL, 2010, *EnergyPlus Engineering Reference*.
- [25] Hellickson M., and Walker J., 1983, *Ventilation of agricultural structures*.
- [26] Monteith J. L., 1973, *Principles of environmental physics*, Edward Arnold, London.
- [27] Bastien D., and Athienitis A. K., 2011, "Transient analysis of Earth-to-air Heat Exchanger for a Home-scale Greenhouse," *Acta horticulturae*, **893**, pp. 477-484.